
UGSL: A Unified Framework for Benchmarking Graph Structure Learning

Bahare Fatemi, Sami Abu-El-Haija, Anton Tsitsulin, Mehran Kazemi,
Dustin Zelle, Neslihan Bulut, Jonathan Halcrow, Bryan Perozzi
Google Research

Abstract

Graph neural networks (GNNs) demonstrate outstanding performance in a broad range of applications. While the majority of GNN applications assume that a graph structure is given, some recent methods substantially expanded the applicability of GNNs by showing that they may be effective even when no graph structure is explicitly provided. The GNN parameters and a graph structure are jointly learned. Previous studies adopt different experimentation setups, making it difficult to compare their merits. In this paper, we propose a benchmarking strategy for graph structure learning using a unified framework. Our framework, called Unified Graph Structure Learning (UGSL), reformulates existing models into a single model. We implement a wide range of existing models in our framework and conduct extensive analyses of the effectiveness of different components in the framework. Our results provide a clear and concise understanding of the different methods in this area as well as their strengths and weaknesses. The benchmark code is available at <https://github.com/google-research/google-research/tree/master/ugsl>.

1 Introduction

Graph Representation Learning (GRL) is a rapidly-growing field applicable in domains where data can be represented as a graph [5]. The allure of GRL models is both obvious and well deserved – there are many examples in the literature where graph structure information can greatly increase task performance (especially when labeled data is scarce) [29, 2]. However, recent results show that the success of graph-aware machine learning models, such as Graph Neural Networks (GNNs), is limited by the quality of the input graph structure [28]. In fact, when the graph structure does not provide an appropriate inductive bias for the task, GRL methods can perform worse than similar models without graph information [5].

As a result, the field of Graph Structure Learning (GSL) has emerged to investigate the design and creation of optimal graph structures to aid in graph representation learning tasks. The relational biases found through GSL typically use multiple different sources of information and can offer significant improvements over the kinds of ‘in vivo’ graph structure found by measuring a single real-world process (*e.g.*, friend formation in a social network). To this end, GSL is especially important in real-world settings where the observed graph structure might be noisy, incomplete, or even unavailable [17].

In this paper, we aim to provide the first holistic examination of Graph Structure Learning. We propose a benchmarking strategy for GSL using a unified framework, which we call Unified Graph Structure Learning (UGSL). The framework reformulates ten existing models into a single architecture, allowing for the first comprehensive comparison of methods. We implement a wide range of existing models in our framework and conduct extensive analyses of the effectiveness of different components in the

framework. Our results provide a clear and concise understanding of the different methods in this area as well as their strengths and weaknesses.

Contributions. Specifically, our contributions are the following: (1) **UGSL**, our unified framework for benchmarking GSL which encompasses over ten existing methods and four thousand different architectures in the same model. (2) **GSL benchmarking study**, the results of our GSL Benchmarking study, a first-of-its-kind effort that compared over *four thousand architectures* across six different datasets in twenty-two different settings, giving insights into the general effectiveness of the components and architectures. (3) **Open source code**, we have open-sourced our code at the following link: <https://github.com/google-research/google-research/tree/master/ugs1> allowing other researchers to reproduce our results, build on our work, and use our code to develop their own GSL models.

2 Preliminaries

Lowercase letters (*e.g.*, n) denote scalars. Bold uppercase (*e.g.*, \mathbf{A}) denotes matrices. Calligraphic letters (*e.g.*, \mathcal{X}) denote sets. Sans-serif (*e.g.*, MyFunc) denotes functions. \mathbf{I} is the identity matrix. For a matrix \mathbf{M} , we represent its i^{th} row as M_i and the element at the i^{th} row and j^{th} column as M_{ij} .

Further, \odot denotes Hadamard product, \circ denotes function composition, Cos is cosine similarity of the input vectors, σ denotes element-wise non-linearity, $^\top$ a transposition operation, and \parallel is a concatenation operation. We let $|\mathcal{M}|$ represent the number of elements in \mathcal{M} and $\|\mathbf{M}\|_F$ indicate the Frobenius norm of matrix \mathbf{M} . Finally, $[n] = \{1, 2, \dots, n\}$.

Let graph $\mathcal{G} = (\mathbf{X}, \mathbf{A})$ be a graph with n nodes, feature matrix $\mathbf{X} \in \mathbb{R}^{n \times d}$, and adjacency matrix $\mathbf{A} \in \mathbb{R}^{n \times n}$. Let in-degree diagonal matrix $\overleftarrow{\mathbf{D}}$ with $\overleftarrow{\mathbf{D}}_{ii}$ counting the in-degrees of node $i \in [n]$, and $\overrightarrow{\mathbf{D}}_{ii}$ counting its out-degree. Let $\mathcal{G} = \mathcal{X} \times \mathcal{A}$ denote the space of graphs with n nodes. Let $\mathcal{G}^{(0)} = (\mathbf{X}^{(0)}, \mathbf{A}^{(0)}) \in \mathcal{G}$ be an **input** graph with feature matrix $\mathbf{X}^{(0)} \in \mathcal{X} \subseteq \mathbb{R}^{n \times d_0}$ and adjacency matrix $\mathbf{A}^{(0)} \in \mathcal{A} \subseteq \mathbb{R}^{n \times n}$. In most-cases, $\mathbf{X}^{(0)} = \mathbf{X}$ (and $d_0 = d$).

The **Graph Structured Learning (GSL) problem** is defined as follows: *Given $\mathcal{G}^{(0)}$ and a task T find an adjacency matrix \mathbf{A} which provides the best graph inductive bias for T .* Our proposed method UGSL captures functions of the form: $f : \mathcal{G} \rightarrow \mathcal{G}$, where f denotes a graph generator model. Specifically, we are interested in methods that (iteratively) output graph structures as:

$$\mathcal{G}^{(\ell)} = (\mathbf{X}^{(\ell)}, \mathbf{A}^{(\ell)}) = f^{(\theta_{\ell, \ell})}(\mathbf{X}^{(\ell-1)}, \mathbf{A}^{(\ell-1)}) \quad \text{for } \ell \in [L] \quad \text{with } f^{(\theta)} = f^{(\theta_{L, L})} \circ \dots \circ f^{(\theta_{1, 1})} \quad (1)$$

Here, $f^{(\theta_{\ell, \ell})}$ represents the ℓ -th graph generator model with parameters θ_{ℓ} . A variety of methods fit this framework. A class of these methods does not process an adjacency matrix as input. As such, they can be written as $f^{(\theta)} : \mathcal{X} \rightarrow \mathcal{X} \times \mathcal{A}$. Another class does not output node features, *i.e.*, $f^{(\theta)} : \mathcal{X} \times \mathcal{A} \rightarrow \mathcal{A}$. Nonetheless, we only consider f with $\mathcal{A} \in \text{range}(f)$. Specifically, methods that output an adjacency matrix.

It is worth stating that some classical methods *e.g.*, k -nearest neighbors (k NN) and partial SVD, fit this framework, both with $L = 1$. Specifically, one can define $\mathbf{X}^{(0)}$ as given features and $f^{(1)}$ for k -NN to output adjacency matrix $\mathbf{A}^{(k\text{NN})} = f^{(1)}(\mathbf{X}^{(0)})$ as

$$\mathbf{A}_{ij}^{(k\text{NN})} = 1 \iff j \in \text{NearestNeighbors}_k(i), \quad (2)$$

where $\text{NearestNeighbors}_k(i) \subseteq [n]^k$ is k -nearest neighbors to i , per a distance function, *e.g.*, Euclidean distance. For partial SVD, one can set $\mathbf{A}^{(0)} = \mathbf{A}$ and set:

$$\mathbf{A}^{(\text{PARTIALSVD})} = f^{(1)}(\mathbf{A}^{(0)}) = \mathbf{U}_* \mathbf{V}_*^\top \quad (3)$$

$$\text{where } \mathbf{U}_*, \mathbf{V}_* = \arg \min_{\mathbf{U}, \mathbf{V}} \left\| \left(\mathbf{U} \mathbf{V}^\top - \mathbf{A}^{(0)} \right) \odot \mathbf{1}[\mathbf{A}^{(0)} > 0] \right\|_F \quad (4)$$

Beyond fitting classical algorithms into UGSL, we are interested in unifying modern algorithms that infer the adjacency matrix with complex processes, *e.g.*, via a deep neural network. Further, we are interested in methods where the adjacency matrix produced by f is utilized in a downstream model, which can be trained in a supervised, unsupervised, or self-supervised, end-to-end manner.

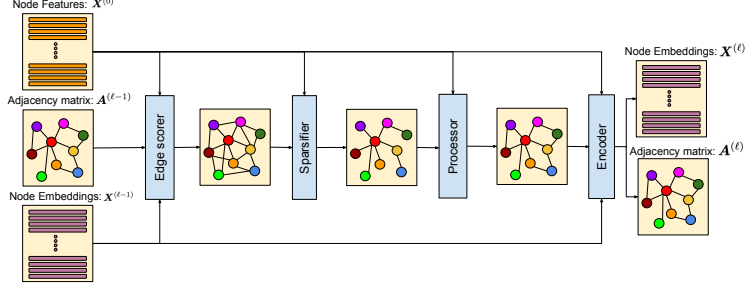


Figure 1: Overview of the ℓ -th GSL layer, $f^{(\ell, \theta^\ell)}$.

3 UGSL: A Unified Framework for Graph Structure Learning Models

The objective of this section is to present a comprehensive unified framework for models designed for graph structure learning. We first describe our proposed unified framework using UGSL layers, a general layer for graph structure learning. The ℓ -th UGSL layer defines function $f^{(\ell, \theta^\ell)}$ as:

$$f^{(\ell, \theta^\ell)} = \text{Encoder}^{(\theta_E^\ell)} \circ \text{Processor}^{(\theta_P^\ell)} \circ \text{Sparsifier}^{(\theta_S^\ell)} \circ \text{EdgeScorer}^{(\theta_{ES}^\ell)}, \quad (5)$$

the composition of 4 trainable modules. Multiple UGSL layers can be combined to create a UGSL model as in Equation 1. Next, we summarize the role of each module. Then, we show that many methods can be cast into the UGSL framework by specifying these modules (Table 7).

* Input: Each UGSL layer ℓ takes as input the output graph of the $(\ell - 1)$ -th layer $G^{(\ell-1)} = (\mathbf{X}^{(\ell-1)}, \mathbf{A}^{(\ell-1)})$, and the input graph $G^{(0)} = (\mathbf{X}^{(0)}, \mathbf{A}^{(0)})$.

* EdgeScorer (w. parameters θ_{ES}) scores every¹ node-pair, producing output $\in \mathbb{R}^{n \times n}$.

$$\mathbf{A}^{(ES, \ell)} = \text{EdgeScorer}(G^{(0)}, G^{(\ell-1)}; \theta_{ES}) \quad (6)$$

* Sparsifier (w. parameters θ_S) Sparsifies the graph, *e.g.*, via top- k or thresholding:

$$\mathbf{A}^{(S, \ell)} = \text{Sparsifier}(G^{(0)}, G^{(\ell-1)}, \mathbf{A}^{(ES, \ell)}; \theta_S) \quad (7)$$

* Processor (w. parameters θ_P) takes the output of the sparsifier and output a processed graph as:

$$\mathbf{A}^{(P, \ell)} = \text{Processor}(G^{(0)}, G^{(\ell-1)}, \mathbf{A}^{(S, \ell)}; \theta_P) \quad (8)$$

* Encoder (w. parameters θ_E) generates updated node embeddings $\mathbf{A}^{(E, \ell)}$ as:

$$G^{(\ell)} = (\mathbf{X}^{(\ell)}, \mathbf{A}^{(E, \ell)}) = \text{Encoder}(G^{(0)}, G^{(\ell-1)}, \mathbf{A}^{(P, \ell)}; \theta_E) \quad (9)$$

* Output: The above modules are invoked for $\ell \in [L]$ giving final UGSL output of:

$$G^{(L)} = (\mathbf{X}^{(L)}, \mathbf{A}^{(E, L)}). \quad (10)$$

4 Experimental Design

We ablate a variety of choices for modules introduced in §3 over six datasets from various domains. Overall, we run hundreds of thousands of experiments, exploring module choices and hyperparameters. We conduct two kinds of explorations: line search (§4.1) and random search (§4.2).

¹Naive all-pairs require $\mathcal{O}(n^2)$ though can be approximated with hashing with $\mathcal{O}(n)$ resources.

Positional encoding	Explanation
WL role	Positional encoding based on the Weisfeiler-Lehman absolute role [33].
Spectral role	Positional encoding based on the top k eigenvectors of the graph laplacian.

Table 1: An Overview of Different Positional Encodings.

Datasets. To benchmark using the UGSL framework, we experiment across six different datasets from various domains. The first class of datasets consists of the three established benchmarks in the GNN literature namely Cora, Citeseer, and Pubmed [31]. Another dataset is Amazon Photos (or Photos for brevity) [32] which is a segment of the Amazon co-purchase graph [26]. The other two datasets are used extensively for classification with no structure known in advance. One is an image classification dataset Imagenet-20 (or Imagenet for brevity), a subset of Imagenet containing only 20 classes (totaling 10,000 train examples). We used a pre-trained Vision Transformer feature extractor [10]. The last dataset is a text classification dataset Stackoverflow [41]. We used a subset collected by Xu et al. [41] consisting of 20,000 question titles associated with 20 categories. We obtained their node features from a pre-trained Bert [9] model loaded from TensorFlow Hub.

Implementation. The framework and all components are implemented in Tensorflow [1] using the TF-GNN library [13] for learning with graphs.

4.1 Experimenting with Components of UGSL

This section explores the key components of different UGSL modules and experiments with them across various datasets.

Base model. A base model is a UGSL model that is used as a reference for comparisons. The objective of such a model is to be minimal and have popular components. Inspired by dual encoder models for retrieval [15], our base model uses only raw features in the input, has an MLP as edge scorer, k-nearest neighbors as sparsifier, no processor, and a GCN as an encoder with no regularizer or unsupervised loss function. The base model is trained with a supervised classification loss. The components of the base model will be explained as we explore different options for each component.

In the rest of this section, we explain different components of the framework and experiment with them. For analyzing different components, we consider the base model and only change the corresponding component to be able to measure the effectiveness of one component at a time in isolation.

Input. To make our proposed framework applicable to a wide range of applications and conduct coherent experiments on multiple datasets, we assume $A^{(0)}$ is an empty matrix. When a non-empty $A^{(0)}$ is required (e.g., for computing positional encodings), we create a kNN graph from the raw features X . For $X^{(0)}$, many models assume $X^{(0)} = X$, i.e., the input embeddings are simply the given node features. However, in some architectures, $X^{(0)}$ is defined differently to contain information from the input adjacency matrix $A^{(0)}$ too. Here, we explore two approaches one based on positional encodings of the Weisfeiler-Lehman (WL) absolute role of the nodes and another based on positional encodings of top k eigenvectors of the graph Laplacian, both proposed in [46]. We explain the two variants in Table 1 and compare their results in Table 2 (Input rows).

Insight 1: Adding information about the input adjacency matrix to the raw features yields improved performance compared to using raw features, across the five datasets. This holds even on datasets with less expressive raw features, e.g., bag-of-words in Cora and Citeseer.

Edge scorer. Most edge scorers in the literature are variants of one of the following: Full parameterization (FP), Attentive (ATT), and multilayer perceptron (MLP). Table 3 shows a summary of edge scorers. Table 2 (Edge scorer rows) compares the edge scorers across the datasets.

Insight 2: The FP edge scorer outperforms MLP and ATT across the five datasets. The only dataset with ATT outperforming the two others is Imagenet. Imagenet uses a pre-trained Vision Transformer feature extractor [10] and thus has more expressive features compared to the bag of words in Cora and Citeseer and Bert [8] embeddings in Stackoverflow.

Insight 3: For the FP edge scorer, we tried two different methods for initializing the adjacency: using glorot-uniform [16], or initializing each edge based on the cosine similarity of the input

Table 2: Results comparing different components used in UGSL.

	Component	Cora		Citeseer		Pubmed		Photo		Imagenet		Stackoverflow	
		Val	Test	Val	Test	Val	Test	Val	Test	Val	Test	Val	Test
Input	Raw features	68.20	65.30	69.20	67.30	72.60	69.60	80.91	79.87	96.80	94.25	76.28	75.86
	WL Roles	50.60	49.60	38.60	29.90	60.80	58.50	79.87	78.76	96.70	94.35	68.82	69.51
	Spectral Roles	69.60	68.10	69.50	68.10	68.40	67.90	83.40	81.26	96.85	93.55	76.08	76.21
Edge scorer	MLP	68.20	65.30	69.20	67.30	72.60	69.60	80.91	79.87	96.80	94.25	76.28	75.86
	ATT	56.00	53.30	56.60	54.40	68.40	66.50	64.70	63.37	96.60	95.06	61.66	60.21
	FP	69.60	67.70	71.40	69.90	71.80	72.20	86.80	85.80	96.90	94.25	76.73	77.72
Sparsifier	kNN	68.20	65.30	69.20	67.30	72.60	69.60	80.91	79.87	96.80	94.25	76.28	75.86
	ϵ NN	66.20	65.20	64.40	60.60	67.80	66.00	79.87	79.12	78.58	74.60	66.37	65.98
	d-kNN	68.60	68.00	66.40	66.20	73.80	70.10	86.14	84.36	96.75	93.34	76.93	77.12
	Random d-kNN	68.80	65.00	66.80	66.20	72.80	71.40	82.75	82.52	96.90	94.46	77.03	77.34
	Bernoulli relaxation	70.20	45.40	71.20	64.10	66.40	41.30	46.80	45.78	91.06	31.65	57.55	49.00
Processor	none	68.20	65.30	69.20	67.30	72.60	69.60	80.91	79.87	96.80	94.25	76.28	75.86
	symmetrize	67.40	66.80	68.80	65.90	73.60	71.80	88.50	86.80	96.75	94.96	74.17	74.81
	activation	67.80	66.10	68.60	63.00	70.80	69.00	82.09	81.83	96.75	94.96	76.18	75.92
	activation-symmetrize	68.41	67.12	68.23	62.30	73.20	70.30	86.67	86.93	96.75	95.26	77.63	77.83
Encoder	GCN	68.20	65.30	69.20	67.30	72.60	69.60	80.91	79.87	96.80	94.25	76.28	75.86
	GIN	63.80	60.20	63.40	62.01	72.00	71.90	89.41	88.10	96.90	94.05	77.83	77.73
	MLP	54.60	49.60	51.80	50.70	71.60	71.10	89.15	87.16	96.90	94.35	77.23	78.37
Regularizer	none	68.20	65.30	69.20	67.30	72.60	69.60	80.91	79.87	96.80	94.25	76.28	75.86
	closeness	72.00	68.00	71.60	66.30	71.20	70.60	87.19	85.00	96.60	93.55	70.82	71.56
	smoothness	69.20	66.20	71.00	66.60	76.60	72.21	86.54	84.00	96.75	95.06	72.32	70.98
	sparse-connect	69.40	67.50	71.00	67.40	80.60	76.40	86.80	85.93	96.80	94.96	75.42	75.03
	log-barrier	67.80	66.90	61.60	56.00	70.40	66.40	40.39	40.36	96.75	94.25	71.30	72.30
	sparse-connect, log-barrier	72.20	68.60	71.00	67.70	79.20	75.80	83.66	82.84	96.70	94.25	71.72	70.12
Unsupervised loss	none	68.20	65.30	69.20	67.30	72.60	69.60	80.91	79.87	96.8	94.25	76.28	75.86
	denoising loss	72.61	70.21	70.22	65.71	67.64	64.80	78.30	77.57	96.7	94.05	69.87	70.12
	contrastive loss	73.41	71.40	72.25	68.41	79.42	75.70	92.94	91.04	96.9	95.16	73.77	73.71
One or per layer	one adjacency	68.20	65.30	69.20	67.30	72.60	69.60	80.91	79.87	96.80	94.25	76.28	75.86
	per layer adjacency	67.41	65.22	68.21	67.00	71.80	69.90	69.28	70.27	96.70	94.56	73.17	74.33

Edge scorer	Formula	Description
FP	$A_{ij}^{(ES, \epsilon)} = V_{ij}^{(ES)}$	Each possible edge in the graph has a separate parameter learned directly. Initialization $V_{ij}^{(ES)} = \text{Cos}(\mathbf{X}_i^{(0)}, \mathbf{X}_j^{(0)})$ (cosine similarity of features) is significantly better than random.
ATT	$A_{ij}^{(ES, \epsilon)} = \frac{1}{m} \sum_{p=1}^m \text{Cos}(\mathbf{X}_i^{(l-1)} \odot \mathbf{V}_p^{(ES)}, \mathbf{X}_j^{(l-1)} \odot \mathbf{V}_p^{(ES)})$	Learning a multi-head version of a weighted cosine similarity.
MLP	$A_{ij}^{(ES, \epsilon)} = \text{Cos}(\text{MLP}(\mathbf{X}_i^{(l-1)}), \text{MLP}(\mathbf{X}_j^{(l-1)}))$	A cosine similarity function on the output of an MLP model on the input.

Table 3: An overview of different edge scorers.

features of the two nodes. We randomly searched over this hyperparameter (similar to the rest of the hyperparameters). We observed that the cosine-similarity initialization outperforms glorot-uniform.

Sparsifier. Sparsifiers take a dense graph generated by the edge scorer and remove some of the edges. This reduces the memory footprint to store the graph (*e.g.*, in GPU), as well as the computational cost to run the GNN. Here, we experiment with the following sparsifiers: k-nearest neighbors (kNN), dilated k-nearest neighbors (d-kNN), ϵ -nearest neighbors (ϵ NN), and the concrete relaxation [18] of the Bernoulli distribution (Bernoulli). Table 4 summarizes these methods. The results comparing the sparsifiers are summarized in Table 2 (Sparsifier rows).

Insight 4: In the case of ϵ NN, since the number of edges in the graph is not fixed (compared to kNN) and the weights are being learned, the number of edges whose weight surpasses ϵ may be large, and so running ϵ NN on accelerators may cause an out-of-memory error.²

Insight 5: The relaxation of Bernoulli does not generalize well to the test set due to its large fluctuation of loss at train time.

Insight 6: The kNN variants outperform ϵ NN on our datasets. Among the kNN variants, dilated kNN works better than the other variants on five datasets. This is likely because dilation increases the receptive field of each node, allowing it to capture information from a larger region of the graph. This can increase the local smoothness of the node representations by approximating a larger neighborhood, leading to better performance in the downstream task.

²To avoid this issue, we tried ϵ NN on an extensive memory setup.

Sparsifier	Formula	Description
kNN	$\mathbf{A}_{ij}^{(S,\ell)} = \begin{cases} \mathbf{A}_{ij}^{(ES,\ell)} & j \in \{N(i)_0, N(i)_1, \dots, N(i)_k\} \\ 0 & \text{otherwise} \end{cases}$	Define $N(i) = \text{arg sort}_j \mathbf{A}_{ij}^{(ES,\ell)}$. Then, for each node, keep the top k edges with the highest weights.
d-kNN	$\mathbf{A}_{ij}^{(S,\ell)} = \begin{cases} \mathbf{A}_{ij}^{(ES,\ell)} & j \in \{N(i)_0, N(i)_d, \dots, N(i)_{(k-1)d}\} \\ 0 & \text{otherwise} \end{cases}$	Dilated convolutions [44] were introduced in the context of graph learning by [23] to build graphs for very deep graph networks. We adapt dilated nearest neighbor operator to GSL. d-kNN adds a dilation with the rate d to kNN to increase the receptive field of each node.
ϵ NN	$\mathbf{A}_{ij}^{(S,\ell)} = \begin{cases} \mathbf{A}_{ij}^{(ES,\ell)} & \mathbf{A}_{ij}^{(ES,\ell)} > \epsilon \\ 0 & \text{otherwise} \end{cases}$	Only keeping the edges with weights greater than ϵ .
Bernoulli	$\tilde{\mathbf{A}}_{ij}^{(S,\ell)} = \text{Sigmoid} \left(\frac{1}{t} \left(\log \frac{\mathbf{A}_{ij}^{(ES,\ell)}}{1 - \mathbf{A}_{ij}^{(ES,\ell)}} + \log \frac{a}{1-a} \right) \right)$	Applying a relaxation of Bernoulli. Following [35], we only keep the edges with weights greater than ϵ (ϵ NN). Alternatively, the regularizer proposed in [27] can be used to encourage sparsity.

Table 4: An overview of different sparsifiers.

Processor	Formula	Description
symmetrize	$\mathbf{A}_{ij}^{(P,\ell)} = \frac{\mathbf{A}_{ij}^{(S,\ell)} + \mathbf{A}_{ji}^{(S,\ell)}}{2}$	Making a symmetric version from the output of sparsifier.
activation	$\mathbf{A}_{ij}^{(P,\ell)} = \sigma(\mathbf{A}_{ij}^{(S,\ell)})$	A non-linear function σ is applied on the output of sparsifier.
activation-symmetrize	$\mathbf{A}_{ij}^{(P,\ell)} = \frac{\sigma(\mathbf{A}_{ij}^{(S,\ell)}) + \sigma(\mathbf{A}_{ji}^{(S,\ell)})}{2}$	First applying a non-linear transformation and then symmetrizing the output.

Table 5: An overview of different processors.

Processor. Many works in the literature have explored the use of different forms of processing on the output of sparsifiers. These processing techniques can be broadly classified into three categories: i. applying non-linearities on the edge weights, *e.g.*, to remove negative values, ii. symmetrizing the output of sparsifiers, *i.e.*, adding edge $v_j \rightarrow v_i$ if $v_i \rightarrow v_j$ survived sparsification, and iii. applying both (i.) and (ii.). The processors we used are listed in Table 5 and the results of applying these processors are shown in Table 2 (Processor rows).

Insight 7: Both activation (i.) and symmetrization (ii.) help improve the results, and their combination (iii.) performs best on several of the datasets.

Encoder. In this work, we experiment with GCN [22] and GIN [42] as encoder layers that can incorporate the learned graphs. As a baseline, we also add an MLP model that ignores the generated graph and only uses the features to make predictions. The results comparing the encoders are shown in Table 2 (Encoder rows).

Insight 8: On some of the datasets, the GNN variants GCN and GIN outperform MLP by a large margin. In some other datasets, MLP performs on par with the UGSL models.

Insight 9: On datasets with a strong MLP baseline, GIN outperforms GCN, which shows the importance of self-loops in these classification tasks.

Name	Formula	Description
Supervised loss	$\sum_i \text{CE}(\text{label}_i, \text{pred}_i)$	The supervision from the classification task as a categorical cross-entropy (CE represents the cross-entropy loss and the sum is over labeled nodes).
Closeness	$\ \mathbf{A}^{(0)} - \mathbf{A}\ _{\mathcal{F}}^2$	Discourages deviating from the initial graph.
Smoothness	$\sum_{i,j} \mathbf{A}_{ij} \text{dist}(v_i, v_j)$	Discourages connecting (or putting a high weight on) pairs of nodes with dissimilar initial features.
sparse-connect	$\ \mathbf{A}\ _{\mathcal{F}}^2$	Discourages large edge weights.
Log-Barrier	$-\mathbf{1}^T \log(\mathbf{A}\mathbf{1})$	Discourages low-degree nodes, with an infinite penalty for singleton nodes.
Denoising Auto-Encoder	$\sum_{i,j \in \mathcal{F}} \text{CE}(\mathbf{X}_{ij}, \text{GNN}_{\text{DAE}}(\tilde{\mathbf{X}}, \mathbf{A}))$	Selects a subset of the node features \mathcal{F} , adds noise to them to create $\tilde{\mathbf{X}}$, and then trains a separate GNN to denoise $\tilde{\mathbf{X}}$ based on the learned graph.
Contrastive	$\frac{1}{2n} \left(\sum_i \log \frac{\exp(\text{sim}(\mathbf{X}_i^L, \mathbf{Y}_i^L)/\tau)}{\sum_{j=1}^n \exp(\text{sim}(\mathbf{X}_i^L, \mathbf{Y}_j^L)/\tau)} \right) + \log \frac{\exp(\text{sim}(\mathbf{Y}_i^L, \mathbf{X}_i^L)/\tau)}{\sum_{j=1}^n \exp(\text{sim}(\mathbf{Y}_i^L, \mathbf{X}_j^L)/\tau)}$	Let $G_1 = (\mathbf{X}, \mathbf{A})$ and $G_2 = (\mathbf{X}, \text{combine}(\mathbf{A}^{(0)}, \mathbf{A}))$ (\mathbf{A} is the learned structure and $\mathbf{A}^{(0)}$ is the initial $-\mathbf{I}$ if no initial structure). The combine function is a slow-moving weighted sum of the original and the learned graphs. Then, Let G_1 and G_2 be variants of G_1 and G_2 with noise added to the graph and features. The two views are fed into a GNN followed by an MLP to obtain node features $\mathbf{X}^{(L)}$ and $\mathbf{Y}^{(L)}$, on which the loss is computed.

Table 6: A summary of loss functions (supervised and unsupervised) and regularizers.

Model	Input	Edge scorer	Sparsifier	Processor	Regularizers	Unsupervised Losses
GLCN [19]	features	MLP	none	activation	sparse-connect, closeness, log-barrier	none
JLGCN [36]	features	MLP	none	activation	smoothness	none
DGCNN [38]	features	MLP	kNN	activation	none	none
LDS [14]	features	FP	Bernoulli	none	none	none
IDGL [6]	features	ATT	ϵ NN	activation	sparse-connect, log-barrier	none
Graph-Bert [46]	features, WL and spectral	MLP	none	activation	none	none
GRCN [43]	features	MLP	kNN	none	none	none
SLAPS [12]	features	FP, MLP, ATT	kNN	activation-sym	none	denoising
SUBLIME [25]	features	FP, MLP, ATT	kNN	activation-sym	none	contrastive
VIB-GSL [35]	features	MLP	Bernoulli	none	none	denoising

Table 7: Examples of existing models in the UGSL framework along with components. These models all have a GCN encoder.

Loss Functions and Regularizers. In our framework, we experiment with a supervised classification loss, four different regularizers, and two unsupervised loss functions. See Table 6 for a summary of descriptions. Table 2 (Regularizer and Unsupervised loss rows) compares the regularizers and the two unsupervised losses in the UGSL framework respectively. Other forms of loss functions and regularizers have been tried in GSL. For instance, Wang et al. [37] proposes homophily-enhancing objectives to increase homophily in a given graph or Jin et al. [20] propose to use the nuclear norm of the learned adjacency as a regularizer to discourage higher ranks.

Insight 10: The log-barrier regularizer alone does not achieve effective results and this is mainly because this regularizer alone only encourages a denser adjacency matrix.

Insight 11: The sparse-connect regularizer outperforms the rest of the regularizers by a small margin on almost all datasets.

Insight 12: The unsupervised losses increase the performance of the base model the most. This might mainly be because of the supervision starvation problem studied in the GSL literature [12]. The contrastive loss is the most effective across most of the datasets.

Learning an adjacency per layer. In this experiment, we assessed two experimental UGSL layer setups. The first setup assumed a single adjacency matrix to be learned across different UGSL encoder layers. In the second setup, each UGSL encoder layer had a different adjacency matrix to be learned. The results from this experiment are in Table 2 (One or per layer rows).

Insight 13: Learning different adjacency matrices in each layer does not improve the performance. This finding suggests that the increase in model complexity outweighed the benefits of learning a separate adjacency matrix for each layer.

Examples of Existing GSL Models in UGSL. Up to this point, we have explained the main components of UGSL. In Table 7, we describe some of the existing models along with their corresponding components in UGSL.

4.2 Random Search Over All Components

After gaining insights from the component analyses in Section 4.1, we excluded a few options and performed a random search over all remaining components of the UGSL framework, including their combinations and hyperparameters. We excluded ϵ NN and Bernoulli because they require extensive memory and cannot be run on accelerators. For each dataset, we ran 30,000 trials.

Best results obtained. The trials with the best validation accuracy (val accuracy) are reported in Table 10, along with the corresponding test accuracy and the components in the architecture of the corresponding model. The results show that combining different components from different models further improves the base model. As we are running many trials for each dataset, we excluded the sparsifiers with ϵ variants to be able to run all trials on accelerators.

Insight 14: There is no single best-performing architecture; the best-performing components vary across datasets. This is because different datasets have different characteristics, such as the types of nodes and the features available for those. The fact that there is no single best-performing component suggests that it is important to carefully select the components that are most appropriate for the specific dataset and task at hand.

The best-performing components vary across datasets. However, there are some general trends:

Table 8: Results of the best model obtained from a random search over all components along with the results corresponding to their base model.

WL	Spectral	MLP	FP	ATT	kNN	d-kNN	none	symmetrize	activation	activation-symmetrize
78.58	80.56	80.53	80.92	79.90	80.71	81.01	80.24	80.66	80.77	80.54

Table 9: Results of the best model obtained from a random search over all components along with the results corresponding to their base model.

GCN	GIN	closeness	smoothness	sparseconnect	logbarrier	denoising	contrastive
80.86	80.47	80.55	80.64	80.60	80.66	81.04	80.99

Insight 15: While positional encodings were useful with a simple base architecture, they lost their effectiveness and did not provide additional improvement when using better architectures following an exhaustive search.

Insight 16: The ATT edge scorer is accompanied by a GIN encoder in the architectures where it participated. This further confirms Insight 2 on the ATT edge scorer working better for datasets with more expressive features as GIN better incorporates the self-loop information compared to GCN.

4.2.1 Average of the Best Performing Component

To gain more insights into the effectiveness of each component in the UGSL framework, we first identified the top-performing trials for each component on each dataset. We then computed the average accuracy across all datasets for each component. The results of this experiment are in Tables 8 and 9. For future tasks and datasets, this shows how probable it is for a component to be useful. For instance, d-kNN sparsifier, denoising loss, and contrastive loss achieved an average accuracy of 81.01%, 81.04%, and 80.99% respectively across all datasets.

Insight 17: D-kNN, denoising loss, and contrastive loss are more likely to be effective for a variety of tasks and datasets.

Top-performing components. To get more insights from the different trials, in addition to the best results reported above, we analyze the top 5% performing trials for each component and visualize their results. Figures 2 and 3 show the box charts for different components across Pubmed and Imagenet (the rest in the appendix).

Insight 18: Tuning the choice of components in the final architecture is most important for edge scorer, followed by processor, unsupervised loss, and encoder. Tuning the regularizer and the positional encoding has a relatively lower effect.

Best overall architectures. In this experiment, we iterate over all architectures that were among those selected in the random search on all six datasets. For each dataset, we pick the best results corresponding to that architecture and then compute the average of the best results over all datasets. Table 11 shows the architectures corresponding to the top five test accuracy. This result brings insights into what architectures to explore for future applications of GSL.

Insight 19: The architectures listed in Table 11 mostly use both regularizers and unsupervised losses, which suggests that both are necessary to learn a graph structure.

Dataset	Val Accuracy	Test Accuracy	Input Features	Edge scorer	Sparsifier	Processor	Encoder	Regularizers	Unsupervised Losses
Cora (base)	68.20	65.30	features	MLP	kNN	none	GCN	none	none
Cora (best)	70.80	72.30	features	FP	d-kNN	activation	GCN	none	denoising and contrastive
Citeseer (base)	69.20	67.30	features	MLP	kNN	none	GCN	none	none
Citeseer (best)	72.00	71.20	features	FP	kNN	activation-sym	GCN	closeness	none
Pubmed (base)	72.60	69.60	features	MLP	kNN	none	GCN	none	none
Pubmed (best)	80.80	76.00	features	MLP	d-kNN	activation	GIN	sparse-connect	contrastive
Photo (base)	80.81	79.87	features	MLP	kNN	none	GCN	none	none
Photo (best)	92.55	89.84	spectral	ATT	d-kNN	activation	GIN	sparse-connect	denoising and contrastive
Imagenet (base)	96.80	94.25	features	MLP	kNN	none	GCN	none	none
Imagenet (best)	96.95	94.25	features	FP	kNN	activation	GIN	smoothness	none
Stackoverflow (base)	76.28	75.86	features	MLP	kNN	none	GCN	none	none
Stackoverflow (best)	77.48	77.82	features	ATT	kNN	none	GIN	sparse-connect	none

Table 10: Comparison of best random search models vs. base models

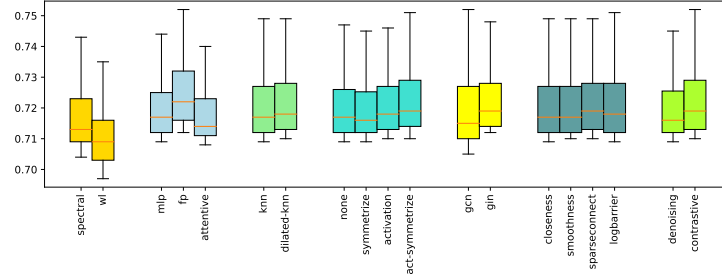


Figure 2: Results of the top 5% performing UGSL models in a random search on Pubmed.

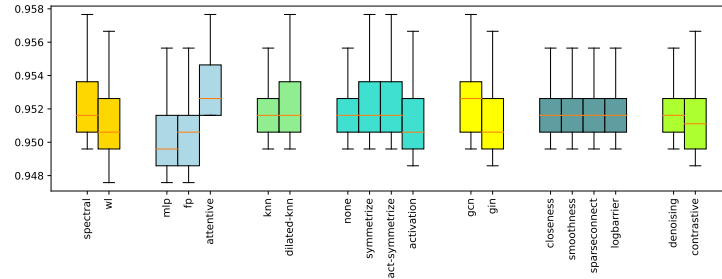


Figure 3: Results of the top 5% performing UGSL models in a random search on Imagenet.

Test Accuracy	Input	Edge scorer	Sparsifier	Processor	Encoder	Regularizers	Unsupervised Losses
75.99	features	FP	kNN	none	GCN	closeness, sparse-connect	contrastive
75.92	features	FP	d-kNN	symmetrize	GIN	none	contrastive
75.71	features	FP	kNN	activation	GIN	none	contrastive
75.63	features	ATT	kNN	symmetrize	GIN	closeness, smoothness, log-barrier	denoising, contrastive
75.60	features	ATT	kNN	symmetrize	GIN	closeness, log-barrier	contrastive

Table 11: Top five performing architectures over the six datasets.

Insight 20: GIN encoders participated in most of the top architectures, showing that using more expressive GNN layers helps even when learning a graph structure at the same time as learning the supervised task.

Insight 21: The ATT edge scorer was not effective most of the time in the base model, but it participated in some of the best architectures, which confirms the importance of searching over all combinations.

Analyses of the graph structures. We further analyze the learned graph structures by computing graph statistics used in GraphWorld [28] (full descriptions in the Appendix), hoping to find correlations between graph structures learned by GSL methods and their downstream quality. Surprisingly, we observe little to no correlation $|\rho| \leq 0.1$ to both validation and test set performance with most metrics. Two metrics did have a limited effect on downstream classification performance: the number of nodes that have degree 1 ($\rho \approx -0.15$) and the overall diameter of the graph ($\rho \approx 0.2 - 0.3$). Degree-one nodes make it difficult for GNNs to pass messages leading to poor performance, however, the case for the diameter of the graph is much less clear and warrants further investigation.

5 Discussions and Future Directions

Graph Structure Learning (GSL) is a rapidly evolving field with many promising future directions. Here are some potential areas for future research.

Scalability. GSL becomes intractable for large number of nodes, as the number of possible edges in a graph grows quadratically with the number of nodes. One family of approaches to this is to utilize approximate nearest neighbor (ANN) search. ANN can mine ‘closest’ pairs of points in time approximately linear in the number of nodes, where ‘close’ is traditionally defined as within some

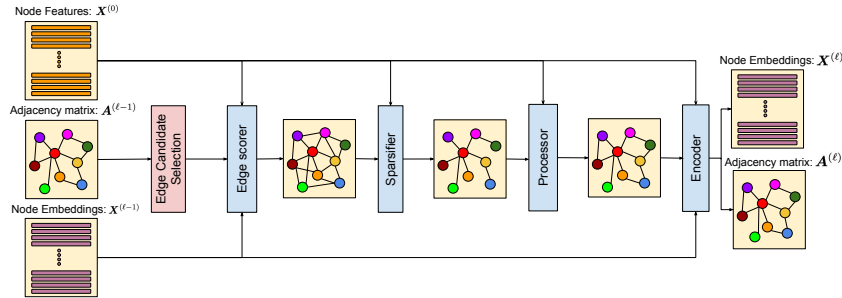


Figure 4: Overview of the l -th scalable GSL layer.

similarity threshold ϵ or within the top- k neighbors of each point. ANN is a well studied problem with a number of approaches developed over the years *e.g.*, [17, 4]. The main limitation to this approach is that the ANN search is not differentiable. Instead these approaches must rely on some heuristic to guide the ANN search. Another family of approaches attempt to scale up graph transformers [45][11]. Nodeformer [40] addresses the scalability issue by kernelizing its similarity function using random feature maps, reducing the complexity of the full message passing step from $\mathcal{O}(N^2)$ to $\mathcal{O}(N)$. It further addresses the associated issue of differentiability with the Gumbel-Softmax reparameterization trick. GraphGPS [30] uses a combination of a message passing neural network with a transformer and considers a few different sparse transformer options such as Performer [7]. However it generally found that these options underperformed a standard transformer. Exphormer [34] adapts the framework from GraphGPS and combines local attention over a graph with global attention and attention over a random expander graph. While some techniques have improved the scalability of graph transformers, these techniques have yet to be shown to be effective for large scale graphs. We consider adapting our framework to larger scale datasets to be future work (Figure 4).

Analyses of the graph structures. One promising future direction is to develop new graph statistics that are more informative about the downstream quality of GSL methods. This could be done by identifying graph properties that are particularly important for GNNs, such as the presence of high-degree nodes or the absence of degree-one nodes, as done for natural graphs by Li et al. [24]. Another important direction for future research is to investigate the relationship between the diameter of the graph and downstream performance in more detail. It is not clear why the diameter of the graph has a limited effect on downstream classification performance, but this could be because GNNs can learn long-range dependencies even in graphs with large diameters.

UGSL beyond node classification. In this work, we primarily focus on the node classification problem, which is the most popular task in the GSL literature (with the exception of some works such as graph classification in [35]). However, since the output of a GSL model is node embeddings, we can use loss functions other than node classification (*e.g.*, link prediction, graph classification, etc.) to guide the learning towards those tasks.

Conclusions. In this paper, we presented UGSL, a unified framework for benchmarking GSL. UGSL encompasses over ten existing methods and four-thousand architectures in the same model, making it the first of its kind. We also conducted a GSL benchmarking study, comparing different GSL architectures across six different datasets in twenty-two different settings. Our findings provide insights about which components performed best both in isolation and also in a large random search. Overall, our work provides a valuable resource for the GSL community. We hope that UGSL will serve as a benchmark for future research and that our findings will help researchers to design more effective GSL models.

References

- [1] Martín Abadi, Ashish Agarwal, Paul Barham, Eugene Brevdo, Zhifeng Chen, Craig Citro, Greg S. Corrado, Andy Davis, Jeffrey Dean, Matthieu Devin, Sanjay Ghemawat, Ian Goodfellow, Andrew Harp, Geoffrey Irving, Michael Isard, Yangqing Jia, Rafal Jozefowicz, Lukasz Kaiser, Manjunath Kudlur, Josh Levenberg, Dandelion Mané, Rajat Monga, Sherry Moore, Derek Murray, Chris Olah, Mike Schuster, Jonathon Shlens, Benoit Steiner, Ilya Sutskever, Kunal

- Talwar, Paul Tucker, Vincent Vanhoucke, Vijay Vasudevan, Fernanda Viégas, Oriol Vinyals, Pete Warden, Martin Wattenberg, Martin Wicke, Yuan Yu, and Xiaoqiang Zheng. TensorFlow: Large-scale machine learning on heterogeneous systems, 2015. URL <https://www.tensorflow.org/>. Software available from tensorflow.org.
- [2] Sami Abu-El-Haija, Bryan Perozzi, Amol Kapoor, Nazanin Alipourfard, Kristina Lerman, Hrayr Harutyunyan, Greg Ver Steeg, and Aram Galstyan. MixHop: Higher-order graph convolutional architectures via sparsified neighborhood mixing. In Kamalika Chaudhuri and Ruslan Salakhutdinov, editors, *Proceedings of the 36th International Conference on Machine Learning*, volume 97 of *Proceedings of Machine Learning Research*, pages 21–29. PMLR, 09–15 Jun 2019. URL <https://proceedings.mlr.press/v97/abu-el-haija19a.html>.
 - [3] Yoshua Bengio, Nicholas Léonard, and Aaron Courville. Estimating or propagating gradients through stochastic neurons for conditional computation. *arXiv preprint arXiv:1308.3432*, 2013.
 - [4] CJ Carey, Jonathan Halcrow, Rajesh Jayaram, Vahab Mirrokni, Warren Schudy, and Peilin Zhong. Stars: Tera-scale graph building for clustering and graph learning. In *International conference on machine learning*, 2022.
 - [5] Ines Chami, Sami Abu-El-Haija, Bryan Perozzi, Christopher Ré, and Kevin Murphy. Machine learning on graphs: A model and comprehensive taxonomy. *Journal of Machine Learning Research*, 23(89):1–64, 2022.
 - [6] Yu Chen, Lingfei Wu, and Mohammed Zaki. Iterative deep graph learning for graph neural networks: Better and robust node embeddings. In *Advances in Neural Information Processing Systems*, volume 33, pages 19314–19326, 2020.
 - [7] Krzysztof Choromanski, Valerii Likhoshesterov, David Dohan, Xingyou Song, Andreea Gane, Tamas Sarlos, Peter Hawkins, Jared Davis, Afroz Mohiuddin, Lukasz Kaiser, et al. Rethinking attention with performers. *arXiv preprint arXiv:2009.14794*, 2020.
 - [8] Jacob Devlin, Ming-Wei Chang, Kenton Lee, and Kristina Toutanova. Bert: Pre-training of deep bidirectional transformers for language understanding. *arXiv preprint arXiv:1810.04805*, 2018.
 - [9] Jacob Devlin, Ming-Wei Chang, Kenton Lee, and Kristina Toutanova. Bert: Pre-training of deep bidirectional transformers for language understanding. *arXiv preprint arXiv:1810.04805*, 2018.
 - [10] Alexey Dosovitskiy, Lucas Beyer, Alexander Kolesnikov, Dirk Weissenborn, Xiaohua Zhai, Thomas Unterthiner, Mostafa Dehghani, Matthias Minderer, Georg Heigold, Sylvain Gelly, Jakob Uszkoreit, and Neil Houlsby. An image is worth 16x16 words: Transformers for image recognition at scale. *ICLR*, 2021.
 - [11] Vijay Prakash Dwivedi and Xavier Bresson. A generalization of transformer networks to graphs. *arXiv preprint arXiv:2012.09699*, 2020.
 - [12] Bahare Fatemi, Layla El Asri, and Seyed Mehran Kazemi. Slaps: Self-supervision improves structure learning for graph neural networks. In *Advances in Neural Information Processing Systems*, volume 34, pages 22667–22681, 2021.
 - [13] Oleksandr Ferludin, Arno Eigenwillig, Martin Blais, Dustin Zelle, Jan Pfeifer, Alvaro Sanchez-Gonzalez, Sibon Li, Sami Abu-El-Haija, Peter Battaglia, Neslihan Bulut, et al. Tf-gnn: graph neural networks in tensorflow. *arXiv preprint arXiv:2207.03522*, 2022.
 - [14] Luca Franceschi, Mathias Niepert, Massimiliano Pontil, and Xiao He. Learning discrete structures for graph neural networks. In *International conference on machine learning*, pages 1972–1982. PMLR, 2019.
 - [15] Daniel Gillick, Alessandro Presta, and Gaurav Singh Tomar. End-to-end retrieval in continuous space, 2018.

- [16] Xavier Glorot and Yoshua Bengio. Understanding the difficulty of training deep feedforward neural networks. In *Proceedings of the thirteenth international conference on artificial intelligence and statistics*, pages 249–256. JMLR Workshop and Conference Proceedings, 2010.
- [17] Jonathan Halcrow, Alexandru Mosoi, Sam Ruth, and Bryan Perozzi. Grale: Designing networks for graph learning. In *Proceedings of the 26th ACM SIGKDD International Conference on Knowledge Discovery & Data Mining*, pages 2523–2532, 2020.
- [18] Eric Jang, Shixiang Gu, and Ben Poole. Categorical reparameterization with gumbel-softmax. *arXiv preprint arXiv:1611.01144*, 2016.
- [19] Bo Jiang, Ziyang Zhang, Doudou Lin, Jin Tang, and Bin Luo. Semi-supervised learning with graph learning-convolutional networks. In *Proceedings of the IEEE/CVF conference on computer vision and pattern recognition*, pages 11313–11320, 2019.
- [20] Wei Jin, Yao Ma, Xiaorui Liu, Xianfeng Tang, Suhang Wang, and Jiliang Tang. Graph structure learning for robust graph neural networks. In *Proceedings of the 26th ACM SIGKDD international conference on knowledge discovery & data mining*, pages 66–74, 2020.
- [21] Diederik P Kingma and Jimmy Ba. Adam: A method for stochastic optimization. *arXiv preprint arXiv:1412.6980*, 2014.
- [22] Thomas N. Kipf and Max Welling. Semi-supervised classification with graph convolutional networks. In *ICLR*, 2017.
- [23] Guohao Li, Matthias Muller, Ali Thabet, and Bernard Ghanem. Deepgcn: Can gcn go as deep as cnns? In *Proceedings of the IEEE/CVF international conference on computer vision*, pages 9267–9276, 2019.
- [24] Ting Wei Li, Qiaozhu Mei, and Jiaqi Ma. A metadata-driven approach to understand graph neural networks. *3rd Workshop on Graph Learning Benchmarks at KDD*.
- [25] Yixin Liu, Yu Zheng, Daokun Zhang, Hongxu Chen, Hao Peng, and Shirui Pan. Towards unsupervised deep graph structure learning. In *Proceedings of the ACM Web Conference 2022*, pages 1392–1403, 2022.
- [26] Julian McAuley, Christopher Targett, Qinfeng Shi, and Anton Van Den Hengel. Image-based recommendations on styles and substitutes. In *Proceedings of the 38th international ACM SIGIR conference on research and development in information retrieval*, pages 43–52, 2015.
- [27] Siqi Miao, Mia Liu, and Pan Li. Interpretable and generalizable graph learning via stochastic attention mechanism. In *International Conference on Machine Learning*, pages 15524–15543. PMLR, 2022.
- [28] John Palowitch, Anton Tsitsulin, Brandon Mayer, and Bryan Perozzi. Graphworld: Fake graphs bring real insights for gnns. In *Proceedings of the 28th ACM SIGKDD Conference on Knowledge Discovery and Data Mining*, KDD ’22, page 3691–3701, New York, NY, USA, 2022. Association for Computing Machinery. ISBN 9781450393850. doi: 10.1145/3534678.3539203. URL <https://doi.org/10.1145/3534678.3539203>.
- [29] Bryan Perozzi, Rami Al-Rfou, and Steven Skiena. Deepwalk: Online learning of social representations. In *Proceedings of the 20th ACM SIGKDD International Conference on Knowledge Discovery and Data Mining*, KDD ’14, page 701–710, New York, NY, USA, 2014. Association for Computing Machinery. ISBN 9781450329569. doi: 10.1145/2623330.2623732. URL <https://doi.org/10.1145/2623330.2623732>.
- [30] Ladislav Rampásek, Michael Galkin, Vijay Prakash Dwivedi, Anh Tuan Luu, Guy Wolf, and Dominique Beaini. Recipe for a general, powerful, scalable graph transformer. *Advances in Neural Information Processing Systems*, 35:14501–14515, 2022.
- [31] Prithviraj Sen, Galileo Namata, Mustafa Bilgic, Lise Getoor, Brian Galligher, and Tina Eliassi-Rad. Collective classification in network data. *AI magazine*, 29(3):93–93, 2008.

- [32] Oleksandr Shchur, Maximilian Mumme, Aleksandar Bojchevski, and Stephan Günnemann. Pitfalls of graph neural network evaluation. *arXiv preprint arXiv:1811.05868*, 2018.
- [33] Nino Shervashidze, Pascal Schweitzer, Erik Jan Van Leeuwen, Kurt Mehlhorn, and Karsten M Borgwardt. Weisfeiler-lehman graph kernels. *Journal of Machine Learning Research*, 12(9), 2011.
- [34] Hamed Shirzad, Ameya Velingker, Balaji Venkatachalam, Danica J Sutherland, and Ali Kemal Sinop. Exphormer: Sparse transformers for graphs. *arXiv preprint arXiv:2303.06147*, 2023.
- [35] Qingyun Sun, Jianxin Li, Hao Peng, Jia Wu, Xingcheng Fu, Cheng Ji, and S Yu Philip. Graph structure learning with variational information bottleneck. In *Proceedings of the AAAI Conference on Artificial Intelligence*, volume 36, pages 4165–4174, 2022.
- [36] Jiayang Tang, Wei Hu, Xiang Gao, and Zongming Guo. Joint learning of graph representation and node features in graph convolutional neural networks. *arXiv preprint arXiv:1909.04931*, 2019.
- [37] Ruijia Wang, Shuai Mou, Xiao Wang, Wanpeng Xiao, Qi Ju, Chuan Shi, and Xing Xie. Graph structure estimation neural networks. In *Proceedings of the Web Conference 2021*, pages 342–353, 2021.
- [38] Yue Wang, Yongbin Sun, Ziwei Liu, Sanjay E Sarma, Michael M Bronstein, and Justin M Solomon. Dynamic graph cnn for learning on point clouds. *Acm Transactions On Graphics (tog)*, 38(5):1–12, 2019.
- [39] Lirong Wu, Haitao Lin, Zihan Liu, Zicheng Liu, Yufei Huang, and Stan Z Li. Homophily-enhanced self-supervision for graph structure learning: Insights and directions. *IEEE Transactions on Neural Networks and Learning Systems*, 2023.
- [40] Qitian Wu, Wentao Zhao, Zenan Li, David Wipf, and Junchi Yan. Nodeformer: A scalable graph structure learning transformer for node classification. In *Advances in Neural Information Processing Systems*, 2022.
- [41] Jiaming Xu, Bo Xu, Peng Wang, Suncong Zheng, Guanhua Tian, and Jun Zhao. Self-taught convolutional neural networks for short text clustering. *Neural Networks*, 88:22–31, 2017.
- [42] Keyulu Xu, Weihua Hu, Jure Leskovec, and Stefanie Jegelka. How powerful are graph neural networks? In *ICLR*, 2019.
- [43] Donghan Yu, Ruohong Zhang, Zhengbao Jiang, Yuexin Wu, and Yiming Yang. Graph-revised convolutional network. In *Machine Learning and Knowledge Discovery in Databases: European Conference, ECML PKDD 2020, Ghent, Belgium, September 14–18, 2020, Proceedings, Part III*, pages 378–393. Springer, 2021.
- [44] Fisher Yu and Vladlen Koltun. Multi-scale context aggregation by dilated convolutions. *arXiv preprint arXiv:1511.07122*, 2015.
- [45] Seongjun Yun, Minbyul Jeong, Raehyun Kim, Jaewoo Kang, and Hyunwoo J Kim. Graph transformer networks. *Advances in neural information processing systems*, 32, 2019.
- [46] Jiawei Zhang, Haopeng Zhang, Congying Xia, and Li Sun. Graph-bert: Only attention is needed for learning graph representations. *arXiv preprint arXiv:2001.05140*, 2020.

A Experimental Design

A.1 Datasets

We ablate various UGSL components and hyperparameters across six different datasets from various domains. The first class of datasets consists of the three established benchmarks in the GNN literature namely Cora, Citeseer, and Pubmed [31]. For these datasets, we only feed the node features to the models **without** their original graph structures (edges). We also experiment with Amazon Photos (or

Table 12: Dataset statistics.

Dataset	Nodes	Edges	Classes	Features	Label rate
Cora	2,708	10,858	7	1,433	0.052
Citeseer	3,327	9,464	6	3,703	0.036
Pubmed	19,717	88,676	3	500	0.003
Amazon-electronics-photo	7,650	143,663	8	745	0.1
Imagenet:20	11,006	0	20	1,024	0.72
Stackoverflow	19,980	0	21	768	0.1

Photos for brevity) [32] which is a segment of the Amazon co-purchase graph [26] with nodes representing goods. We only used the node features for this dataset as well. The other two datasets are used extensively for classification with no structure known in advance. One is an Image classification dataset Imagenet-20 (or Imagenet for brevity), a subset of Imagenet containing only 20 classes (totaling 10,000 train examples). We used a pre-trained Vision Transformer feature extractor [10]. The last dataset is Stackoverflow which is commonly used for short-text clustering/classification tasks. Here, we used a subset collected by Xu et al. [41]. consisting of 20,000 question titles associated with 20 different categories obtained from a dataset released as part of a Kaggle challenge. We obtained their node features from a pre-trained Bert [9] model loaded from TensorFlow Hub. The GitHub repository contains scripts for loading the datasets from their original sources and also computing their embedding using pre-trained models (for Imagenet and Stackoverflow). The statistics of datasets used in the experiments can be found in Table 12.

A.2 Implementation Details.

We implemented the framework with all its components in Tensorflow [1], used the TF-GNN library [13] for learning with graphs operations, and used Adam [21] as optimizer. We performed early stopping and hyperparameter tuning based on the accuracy on the validation set for all datasets.

We fixed the maximum number of epochs to 1,000. We use two layers of UGSL in all the experiments. For the experiments on component analyses, for each dataset and component, we run a search with 1,024 trials. For the random search experiments over all components, we run 30,000 trials for each dataset. We run all our experiments on a single P100 GPU in our internal cluster. For each trial, the hyperparameters are selected randomly from a predefined range (for float hyperparameters) or list (for discrete hyperparameters). The range provided for the learning rate and weight decay of the Adam optimizer are (1e-3, 1e-1) and (5e-4, 5e-2) respectively. All dropout rates and non-linearities are selected from (0.0, 75e-2) and [relu, tanh] respectively. The rest of the hyperparameters are component dependent and are explained in the corresponding section for the component below.

we have open-sourced our code at the following link: <https://github.com/google-research/google-research/tree/master/ugsl>.

A.3 Experimenting with Components of UGSL

In this section, we report charts obtained from the component analyses. These results are summarized in the main paper in spider charts.

Input. Figure 5a shows the spider chart corresponding to the results for feeding raw features as input, incorporating WL roles, and Spectral roles.

Edge scorer. For an MLP edge scorer, the number of layers is selected from the list [1, 2]. It has been mentioned by several recent papers [e.g., 12, 39] in the area that initializing the MLP edge scorer such that it outputs the kNN graph has shown to be promising. For that, we selected hidden size and output size from [500, #features] (500 is changed to 250 for Pubmed with 500 features.). The layers in an MLP edge scorer are either initialized using glorot-uniform [16] or to an identity matrix (having layers of the size #features and initializing the weights as an identity will result in a kNN graph as initialization). The ATT edge scorer weights have been initialized either randomly or to ones (to replicate kNN in the initialization). Figure 5b shows the spider chart corresponding to the charts for comparing three edge scorers MLP, ATT, and FP.

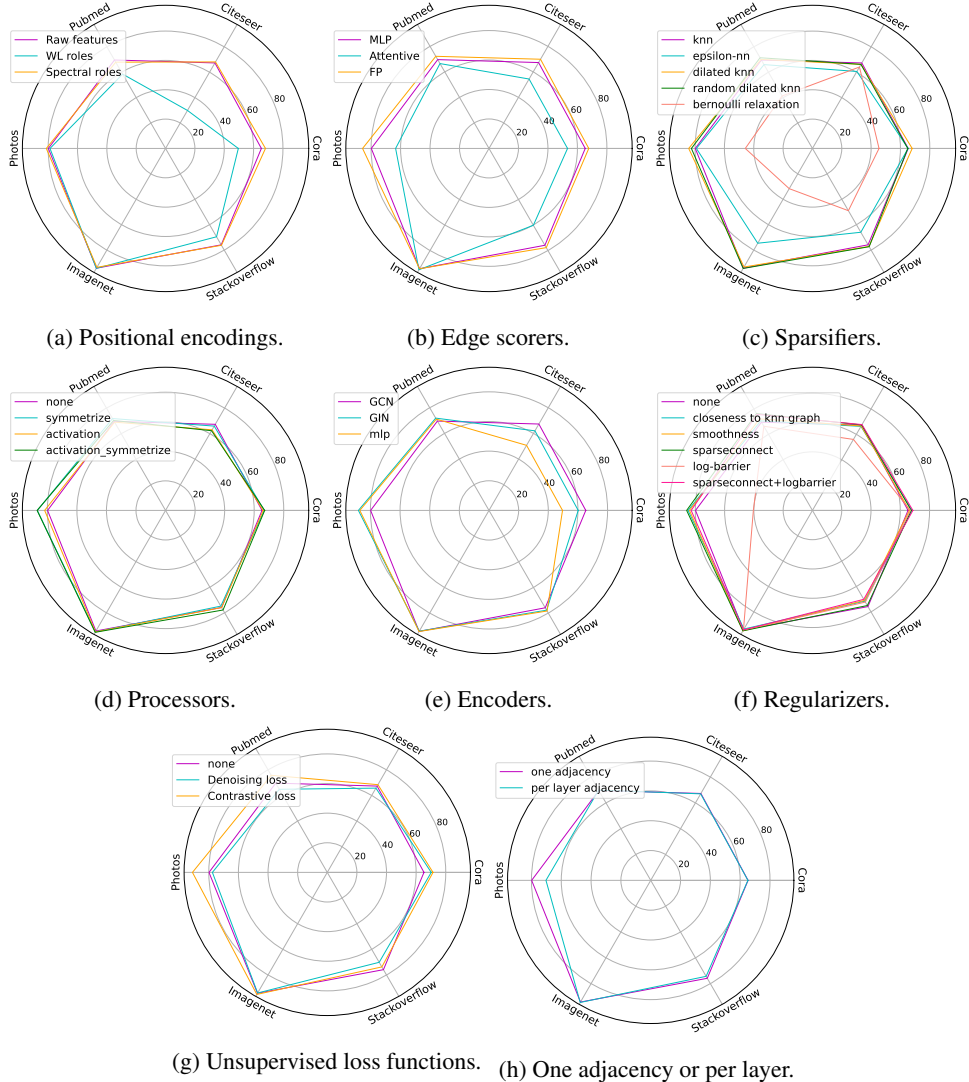


Figure 5: Line-search experiments summarizing thousands of runs. (a-d) ablate UGSL Modules, (e) ablates amending adjacency information into $\mathbf{X}^{(0)}$, (f-g) ablate objective terms, and (h) ablates learning one adjacency or multiple. The raw results are in the appendix.

Sparsifier. The sparsifiers that have kNN variants have their k selected from [15, 20, 25, 30]. d-kNN has a hyperparameter d selected from [2, 3] and a boolean hyperparameter to do random dilation (random d-kNN) or not. The sparsifiers with a hyperparameter as ϵ have it selected from (0.0, 1.0). Figure 5c shows the results for multiple sparsifiers we tried in the architecture.

When using these sparsifiers while learning the parameters of the GSL model, following most of the successful work in this area, we only send gradients toward non-zero values in the output of the sparsifier (e.g., a node being among the top k neighbors in the kNN sparsifier). As discussed in the straight-through estimator proposed by [3], this computes biased gradients, but it works well in practice because it enforces a prior that for a given input, most of the factors in the model are irrelevant and would be represented by zeros in the representation. [3] also investigated multiplying the gradient by the derivative of the sigmoid, but they found that better results were obtained without multiplying the derivative of the sigmoid.

Processor. Figure 5d shows the results for multiple processors we tried in the architecture. The only hyperparameters for the processors are the non-linearity function selected from [relu, tanh].

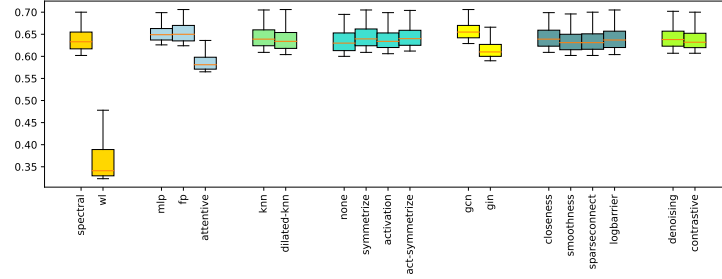


Figure 6: Results of the top 5% performing UGSL models in a random search on Cora.

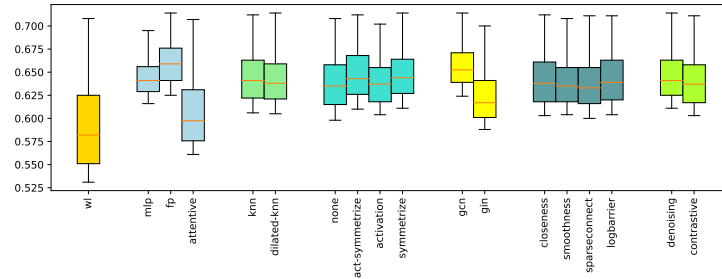


Figure 7: Results of the top 5% performing UGSL models in a random search on Citeseer.

Encoder. The encoder has the number of hidden units as a hyperparameter selected from [16, 32, 64, 128] (non-linearity and dropout rate have been discussed above). Figure 5d shows the results for multiple processors we tried in the architecture.

Loss functions and regularizers. Each regularizer has its own weight selected from (0.0, 20.0). The hyperparameters for the denoising autoencoder and contrastive loss have been optimized based on the suggestions proposed in their corresponding paper. The denoising autoencoder has another GNN inside it with the number of hidden units selected from (512, 1024). The contrastive loss has a mask rate, temperature, and tau selected from (1e-2, 75e-2), (0.1, 1.0), and (0.0, 0.2) respectively. Figure 5f shows the results for multiple regularizers we tried in the architecture. Figure 5g shows the results for the unsupervised loss functions we tried in UGSL.

Learning an adjacency per layer. In this experiment, we assessed two experimental UGSL layer setups. The first setup assumed a single adjacency matrix to be learned across different UGSL encoder layers. In the second setup, each UGSL encoder layer had a different adjacency matrix to be learned. The results from this experiment are in Figure 5h.

A.4 Random Search Over All Components

In this section, we provide more analyses for our extensive random search over all components.

A.4.1 Top-performing Components

To get more insights from the different trials, in addition to the best results reported above, we analyze the top 5% performing trials for each component and visualize their results. The box charts for Pubmed, Photo, Imagenet, and Stackoverflow are in the main paper. Figures 6 and 7 show the box charts corresponding to Cora and Citeseer datasets.

A.5 Analyses of the graph structures

We study graph-level statistics of the constructed graphs using a collection of 7 metrics taken from GraphWorld [28]. Table 13 reports median statistics per dataset and Table 14 contrasts that with statistics of top-1% scoring graphs. We can observe that there are no significant differences across the

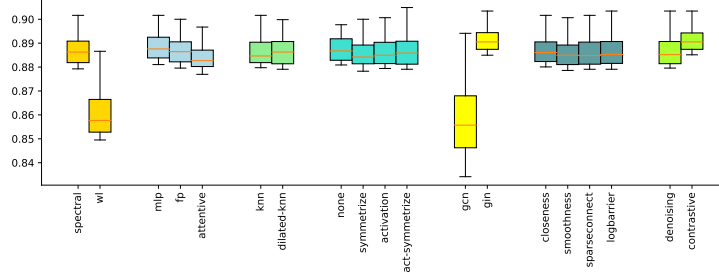


Figure 8: Results of the top 5% performing UGSL models in a random search on Photo.

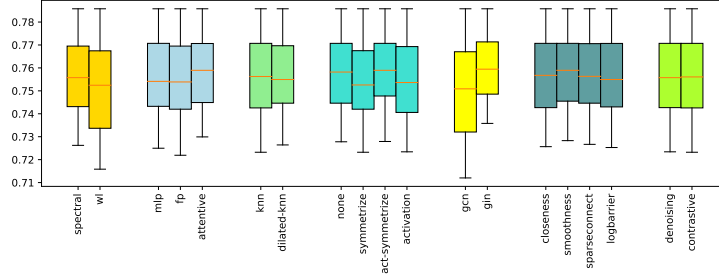


Figure 9: Results of the top 5% performing UGSL models in a random search on Stackoverflow.

best- and average-performing graphs except slightly lower clustering coefficient and higher diameter of best-performing graphs.

Additionally, we compute Spearman rank correlation to the test set accuracies, presented in Table 15. Here, we do not observe significant correlations except the ones reported in the main paper body.

Table 13: Median dataset statistics across all random search trials for all datasets. We report the average node degree \bar{d} , degree power law exponent α , graph diameter, local (\overline{CC}_l) and global (CC_g) clustering coefficients, and graphs' spectral radius $\lambda_{\max}(A)$ and algebraic connectivity $\lambda_2(L)$.

dataset	\bar{d}	α	Diam.	\overline{CC}_l	CC_g	$\lambda_{\max}(A)$	$\lambda_2(L)$
Cora	10.43	1.43	12	0.13	0.05	12.93	0.84
Citeseer	7.15	1.43	13	0.11	0.04	9.45	0.84
Pubmed	5.37	1.50	16	0.17	0.01	7.35	0.86
Photo	8.16	1.41	6	0.25	0.01	13.69	0.85
Imagenet	8.04	1.40	15	0.23	0.12	13.11	0.85
Stackoverflow	8.11	1.41	17	0.15	0.03	12.42	0.87

Table 14: Median dataset statistics for top 1% performing runs.

dataset	\bar{d}	α	Diam.	\overline{CC}_l	CC_g	$\lambda_{\max}(A)$	$\lambda_2(L)$
Cora	10.94	1.41	13	0.10	0.09	13.74	0.84
Citeseer	7.90	1.41	13	0.06	0.06	9.27	0.84
Pubmed	5.28	1.48	17	0.01	0.00	6.04	0.85
Photo	8.01	1.43	9	0.03	0.02	11.93	0.85
Imagenet	9.11	1.39	16	0.22	0.14	14.22	0.85
Stackoverflow	8.17	1.46	19	0.13	0.04	12.08	0.87

Table 15: Spearman rank correlations between dataset statistics and test set accuracies.

<i>dataset</i>	\bar{d}	α	Diam.	$\overline{CC_l}$	CC_g	$\lambda_{\max}(A)$	$\lambda_2(L)$
Cora	0.06	0.22	0.15	0.06	0.16	0.02	-0.10
Citeseer	0.16	0.23	0.20	-0.11	0.02	0.03	-0.18
Pubmed	-0.05	0.09	-0.33	0.29	0.23	0.09	0.34
Photo	-0.08	0.22	-0.15	-0.24	0.04	-0.03	0.08
Imagenet	0.09	-0.03	0.13	0.13	0.23	0.16	0.11
Stackoverflow	-0.02	0.09	0.01	0.06	-0.14	-0.05	0.13